Self-reporting Fiber-Reinforced Composites that Mimic the Ability of Biological Materials to Sense and Report Damage

Omar Rifaie-Graham, Edward A. Apebende, Livia K. Bast and Nico Bruns*

Omar Rifaie-Graham, Edward A. Apebende, Livia K. Bast, Prof. N. Bruns
Adolphe Merkle Institute, University of Fribourg, Chemin des Verdiers 4, 1700 Fribourg, Switzerland
E-mail: nico.bruns@unifr.ch

Abstract

Sensing of damage, deformation and mechanical forces is of vital importance in many applications of fiber-reinforced polymer composites, as it allows to monitor the structural health and integrity of composite components and to detect micro-damages before they lead to catastrophic material failure. This review discusses bio-inspired and bio-mimetic approaches to self-sensing and self-reporting materials. Examples include bruising coatings and bleeding composites based on dye-filled microcapsules, hollow fibers, and vascular networks. Force-induced changes in color, fluorescence or luminescence are achieved by mechanochromic epoxy resins, or by mechanophores and force-responsive proteins located at the interface of glass/carbon fibers and polymers. Composites can also feel strain, stress and damage through embedded optical and electrical sensors, such as fiber Bragg grating sensors, or resistance measurements of dispersed carbon fibers and carbon nanotubes. Bioinspired composites with the ability to show autonomously if and where they have been damaged lead to a multitude of opportunities for aerospace, automotive, civil engineering, and wind turbine applications. They range from safety features for the detection of barely visible impact damage, to the real-time monitoring of deformation of load-bearing components.

1. Introduction

Imagine an animal that does not feel pain. It would be able to perform great feats, although with great risk of permanent damage to its body in terms of overstressed muscles, torn ligaments and more. Thus, feedback mechanisms that report the structural integrity of tissue and body parts are essential for long-term survival. Not surprisingly, a multitude of sensing mechanisms have evolved allowing organisms to assess their health and the state of their body. For example, most tissues in animals

feature a dense array of nerves, which report tissue damage by the sensation of pain. Other means to evaluate whether damage has occurred are optical clues, such as bruises or blood seeping from a wound. These signals allow a timely response to damage and fatigue, be it by reducing stress, further protection of the body or, in the case of humans, seeking medical assistance.

In contrast to the natural world, most materials are passive and do not have the ability to sense, detect and report damage. As a result, the engineering approach to ensure the safe use of materials is to employ a surplus of material, e.g., in load-bearing applications, so that the strength and toughness of the material greatly surpasses any foreseeable forces during its lifetime. In addition, nondestructive testing,[1-3] e.g., by X-ray, ultrasound imaging or lock-in thermography might be carried out at regular intervals to detect microscopic damage before cracks widen and become catastrophic. Last but not least, components can simply be replaced at regular service intervals if their integrity is crucial for the safety of the device, such as in aerospace applications. While these measures help to ensure safe operations, they rely on the use of a surplus of material, which increases weight and therefore fuel consumption, or they involve costly monitoring, repair, and replacement procedures.

Dynamic or static overload, fatigue, and impacts are common causes for damage in polymeric materials. In the context of fiber-reinforced composites, barely visible impact damage (BVID) is of particular relevance. It is caused by low velocity impacts and can occur, e.g., when a technician drops a tool during assembly, service and maintenance to composite structures. The impacting object might not cause more than a small indentation on the surface of the material, but can result in delamination between fiber plies, matrix cracking within a ply, fiber fracture and back-face tensile cracks.[4] Such microdamage may act as a nucleus for larger and potentially hazardous

structural damages. Easy means to detect BVID are therefore of importance to facilitate quality control, especially on large surface areas, so that those spots can be identified that need further inspection, replacement or repair.[5]

Materials that autonomously sense their state and report damage including, but not limited to, BVID have attracted a lot of attention in recent years.[6-10] Those self-reporting (also termed self-sensing or self-monitoring) materials often take inspiration from the biological world, transferring or mimicking the concepts used by nature to sense damage into materials sciences. Often, but not always, self-reporting capabilities go hand in hand with self-healing mechanisms.[11-15] Fiber-reinforced polymer composites are particularly interesting for the implementation of self-sensing mechanisms as they are high performance materials that are often used where lightweight yet strong materials are needed,[16] e.g., in aerospace applications,[17-19] wind turbines,[2, 20, 21] the automotive industry,[22] sporting goods,[23] medicine[24] or in civil engineering.[25, 26] Many of these applications are less cost-sensitive than other applications of polymers, so that the use of smart materials is a viable economic option if it reduces fuel consumption, increases service intervals, or increases safety margins.

Approaches to self-reporting fiber-reinforced composites are summarized in **Figure 1**. Damage and deformation of polymeric materials can be visualized by changes in color, fluorescence or the production of luminescence, in analogy to the warning signals of bruises or bleeding wounds. To achieve such optical signals, dye-filled capsules, hollow fibers or microchannels can be incorporated into damage-indicating coatings, or they can be embedded into the composite, either into the polymer resin or at the interface between fibers and polymer resin.[8, 9, 12-14] Upon rupture of the reservoirs, their content bleeds into cracks and voids, highlighting their location. A

second strategy is to synthesize materials with intrinsic mechanochromic properties.[6-10] To this end, the polymer matrix or the surface of the fibers is functionalized with functional groups, additives or biomacromolecules that change their optical appearance in response to mechanical deformation.

Even though it might appear much more difficult to prepare materials that feel pain than to induce color changes, the implementation of electronic or optic sensing elements into composites is a popular approach for structural health monitoring, especially amongst materials engineers.[20, 21, 27-29] Resistance measuring devices, strain gauges, piezo sensors, optical fiber sensors and other types of deformation sensors can be mounted to the surface of composite components. Alternatively, the sensors can be embedded into the composites during manufacturing. The sensors are connected to data acquisition units and allow to monitor material's properties even over extended periods of times, e.g. in service.

This progress report introduces the reader to the various concepts that are followed to create self-reporting fiber-reinforced composites and critically discusses advantages, drawbacks and future prospects of the approaches by discussing representative examples from the literature. Wherever possible, bioinspired and biomimetic strategies towards self-reporting of damage will be highlighted.

2. Mechanochromic fiber-reinforced composites

2.1 Self-reporting coatings and self-reporting composites based on microcapsules

If a blunt object hits a body, capillaries rupture and release blood into the surrounding interstitial tissue. As a result, a bruise forms. If it is close to the skin, it can be easily observed by the naked eye and is therefore an indication for an accident, a medical problem, or domestic abuse and other forms of violence, even days after the actual incident.

Color changes that report impact damage in materials can be achieved by applying so-called bruising coatings, which have been initially described in patents,[30] e.g., for impact detection on aircraft,[31, 32] and more recently in scientific publications. They are based on a dispersion of dye-filled microcapsules in a coating. Alternatively, dye-filled capsules can be embedded into the bulk of a material. Excellent reviews have summarized the field of microcapsule-based self-reporting (and self-healing) materials.[8, 9, 12-14] In their seminal work, White, Sottos, Moore and coworkers used microcapsules filled with healing agents to prepare self-healing epoxy composites.[33] To visualize the release of healing solution from capsules into damage, a red dye was also encapsulated. As a result, the materials were not only self-healing but also self-reporting. However, there was no color contrast between the dye in the capsules and in the cracks. To increase the contrast between damaged and nondamaged sites, the dye should be colorless when encapsulated but develop or change color or fluoresce when released into the coating. To achieve this effect, pH differences between the dye solution in the capsules and the bulk polymer can be exploited, very similar to the classic working principle of carbonless copy paper.[34] For example, Vidinejev *et al.* encapsulated crystal violet lactone and dispersed the capsules together with the developers methyl 4-hydroxybenzoate or silica gel into an acrylic resin.[35] When bruised, the colorless leuco dye switched to its blue form in the acidic environment provided by the developers. The same group used the combination of microencapsulated leuco dye and acidic developers to render fiber-reinforced composites self-reporting.[36] To this end, nylon fabric was impregnated with a mixture of dye-filled microcapsules, a developer and an epoxy-modified polyurethane–acrylic emulsion, which was cured by UV light to affix the sensing compounds on the fibers. Then, the nylon fabric was laminated as a pressure-sensitive

layer together with load-bearing glass yarn layers into an epoxy resin. The resulting composite showed bruising in response to local indentation, and the force threshold of the color development could be controlled by the thickness of a protecting epoxy layer on top of the sensing layer.

White, Sottos and coworkers recently achieved very high color contrasts in damage-indicating coatings by encapsulating a solution of 2′,7′-dichlorofluorescein in ethylphenyl acetate into double-walled polyurethane/poly(urea–formaldehyde) microcapsules (**Figure 2**).[37] The microcapsules were embedded into an epoxy resin that provided a basic environment through unreacted amine groups of its curing agent. Upon release of the dye into the microcracks, proton exchange between the dye and the amine groups of the epoxy resin caused the dye to switch from its light yellow acidic form to the bright red basic form. As a result, cuts in the coatings can be clearly identified under normal light. Interestingly, its fluorescence was not explicitly exploited in this work. A very important aspect of 2′,7′-dichlorofluorescein is that the color in the damaged areas was highly stable. Its intensity did not decrease within eight months of storage, so that the coating would also indicate damage long after the damaging event happened, which is essential if used as a safety feature.

Other self-reporting dye-filled capsule systems are based on the ring-opening metathesis polymerization of 1,3,5,7-cyclooctatetraene to form a colored conjugated polymer,[38] or spiropyrans that transform into their colored merocyanine form when irradiated with UV light.[39] Self-reporting has also been achieved by a solution of nonfluorescent tetraphenylethylene that starts to fluoresce through aggregation-induced emission once solvent has evaporated from the cracks.[40, 41] Alternatively, a fluorescent liquid within capsules could screen UV irradiation and thereby reduce fluorescence emission from intact microcapsules.[42] The encapsulation of

hexamethylbenzene and chloranil in two sets of microcapsules yielded a self-reporting system that formed red charge-transfer complexes when the compounds met in the deformed polymer matrix.[43]

2.2 Self-reporting composites based on hollow fibers

Microcapsules have only been used in a few cases in the bulk of fiber-reinforced composites, e.g., at the fiber–resin interface.[44] One example of a self-reporting system is the leucodye-containing capsules on nylon fibers that were discussed above.[36] A reason that microcapsules are less popular for the bulk of composites than for nonreinforced plastics might be that it is much easier to use hollow fibers directly as a reservoir for dyes (and self-healing agents) in composites.

The first to release healing agents from glass capillaries into cracks of a polymer matrix was Dry.[45] Also Bleay *et al.* reported hollow glass fibers filled with curing agents as a repairing system for polymer composites.[46] X-ray-opaque dyes were added to the healing solution to facilitate the observation of damage modes by X-radiography, thus making the system self-reporting. Following these early reports, Pang and Bond developed the concept of "bleeding composites" that self-report damage by optical clues and heal damages by the release of healing agents (**Figure 3a**). To this end, hollow glass fibers of 60 μm external diameter were filled with uncured epoxy resin. A second batch of fibers was filled with a mixture of hardener and the fluorescent dye Ardrox 985 which is usually used as a fluorescent penetrant for nondestructive testing in the aerospace sector. Hollow glass fiber/epoxy preimpregnated tapes (prepreg) were produced and hand-laminated together with commercially supplied solid glass fiber/epoxy resin plies into multilayer composites.[47, 48] The fiber-reinforced composites were subjected to low-velocity

impacts and to flexural bending tests, which caused the hollow fibers to break open and release their contents into the damaged area. As a result, hardener and uncured epoxy resin from the hollow fibers came in contact, cured within the cracks and restored the mechanical properties of the composites to a significant extent. Moreover, the fluorescent dye infiltrated damage sites, so that they could be easily located by means of fluorescence imaging, thus allowing for the visual detection of BVID.

Other self-healing and self-reporting composites based on hollow glass fibers, filled with healing agents and an indicator dye, have been reported.[49, 50] Kling and Czigány developed the concept further, by infiltrating much thinner glass capillaries (10–13 μm outer diameter) with polyester resin curing agents and Rhodamine B (Figure 3b).[51] Because of their thin diameter, the hollow fibers could reinforce the resin more efficiently than wider hollow fibers. The resin was colored with a white dye to mask the fluorescent color of the rhodamine in the undamaged capillaries. Upon damage by an impactor, the indicator fluid from the capillaries flowed to the surface, so that damage and self-healing sites could be visualized with the help of a UV lamp.

2.3 Self-reporting composites based on microchannels and vascular networks

While microcapsules and hollow fibers allow creating bruising or bleeding effects, the analogy to natural tissue is not perfect. The liquid that is released from the reservoirs into damage sites leaves behind a void that can lead to reduced mechanical strengths of the healed material. Moreover, the healing and self-indication effect can only occur once at a specific site because the healing and indicating liquid is used up. In contrast, tissue is vascularized by blood vessels through which blood constantly flows. Blood is continuously transported to a lesion until clotting sets in as the first step of the healing process. Moreover, tissue can heal repeated damage at the same location. Not only animals but also plants have channels that transport healing agents.[52] For example, pine trees and some other tree families secrete resin into an interconnected three-

dimensional network of resin canals.[53] If the vascular cambium is damaged, the epithelial cells that line the canals take up water, swell and press the resin toward the damage.[54, 55] Compared with the blood circulation system of animals, the network structure of the resin canals has the benefit that transport can be accomplished even if one channel is interrupted or blocked.[52]

Inspired by the transport in vascular systems, synthetic materials that are vascularized by microchannels have been prepared. Liquid healing agents can be pumped through these channels to damage sites. Often, dyes are added to the self-healing agents to visualize the release of liquid into damage sites, thus creating self-reporting materials.[52] Microvascularized self-healing materials are summarized in excellent recent reviews.[12, 14, 15] Here, selected reports will be highlighted to demonstrate the principle. Amongst the pioneers were once again White, Sottos, Moore and coworkers.[56, 57] They coated a vascularized specimen with an epoxy coating that contained Grubbs' catalyst for ring-opening metathesis polymerization (ROMP). The microchannels were filled with a solution of the monomer dicyclopentadiene. Crack formation in the specimen released the monomer solution and repeatedly cured cracks in the coating by ROMP. In these reports, no dyes were released, so that the materials were self-healing, but not self-reporting.

To integrate vascular channels into the bulk of fiber-reinforced composites, channels must be created either between plies of fiber fabric, or within the fabric itself. A possibility to achieve this is to incorporate sacrificial materials that can be removed during or after curing. Bond, Trask and coworkers have used solder wire with a diameter of 0.25 mm or 0.5 mm for this purpose.[52, 58] It was placed either between plies or within precut recesses within a ply. By heating the material to 190 °C under vacuum after curing, the solder wire was removed, leaving behind vascular channels.

After applying impact damage to the composite, a one-component epoxy/hardener solution was injected into the channels, healing the damage. The solution was further doped with a fluorescent dye to allow for visualization of the damage layout, potentially also allowing for a facile visual damage inspection of large surfaces.

Other possibilities to create sacrificial structures for the vascularization of fiber-reinforced composites are electrospun nonwoven mats of the neutral polysaccharide pullulan that can be dissolved out of the polymer matrix using water,[59] or 3-D printed water-soluble poly(vinyl alcohol).[60] Fibers and wires, such as nylon fibers coated with beeswax as an antiadhesive,[61] or PTFE-coated stainless steel or nickel chromium wires,[62-65] can be pulled out of the composite material after curing to leave behind microchannels.

More advanced designs of microvascular channels confine two components of a self-healing system into two interwoven three-dimensional microvasculatures that are integrated into fiber fabrics. For example, poly(lactic acid) (PLA) filaments that contained tin(II) oxalate as a depolymerization catalyst were stitched into glass fiber fabrics (**Figure 4**).[66] Once embedded into epoxy resin, the PLA filaments were depolymerized and vaporized by thermal treatment in vacuum, leaving behind channels that were then filled with an epoxy prepolymer and with an amine-based hardener. Delamination damage within the composite could be healed repeatedly by delivering resin and hardener with two high-precision fluid dispensers that were connected to the microchannels. To investigate the mixing of the two liquids at damage sites, different fluorescent dyes (nile red and fluorescein) were added to each of the healing agents. The delivery and mixing of the curing and staining agents was more effective when the channels were arranged in a herringbone pattern than when arranged in parallel, as observed by fluorescence imaging. However, the images also

reveal that the mixing of the two healing components was not homogeneous. The targeted stoichiometry of the two healing agents was only achieved in parts of the damaged area. In a recent study, the vascularization by vaporization of sacrificial PLA was further enhanced, as 3-D-interconnected networks of microchannels were created in fiber-reinforced composites by combining PLA fibers and printed PLA structures.[67] Moreover, sacrificial, channel-forming PLA filaments were woven together with glass and carbon fibers into a noncrimp orthogonal pattern using 3-D-weaving machines.[67, 68]

2.4 Self-reporting composites based on mechanophores and mechanochromic additives

2.4.1 Mechanophores and mechanochromic additives

Self-reporting of damage can also be achieved by using polymers that are intrinsically mechanochromic, i.e., that change their color, fluoresce or emit luminescence in response to mechanical forces. This is often achieved by the incorporation of mechanically sensitive functional groups, so-called mechanophores, into the backbone of a polymer.[6-10] The polymer chains transduce mechanical forces onto a labile bond within the mechanophore, causing it to react or rearrange. Popular mechanophores and the mechanism of their mechanically induced color, fluorescence or luminescence changes are summarized in **Table 1**. Among the most prominent examples are spiropyrans.[69] When stressed, they undergo a conformational rearrangement to the merocyanin form, which is colored and fluorescent. Materials that have been made mechanochromic by spiropyrans include poly(methyl acrylate),[70, 71] polydimethylsiloxane,[72] silicone rubbers that indicate local compression[73] or that develop fluorescence in response to an electrical field,[74] rubber toughened poly(methyl methacrylate),[75, 76] polystyrene coatings that produce optical changes when subjected to shockwaves,[77] self-reporting and self-healing

supramolecular systems,[78, 79] and 3-D printed materials.[80] Other mechanochromic molecules that have been incorporated into polymers include the color changing cyano oligo(*p*-phenylene vinylenes),[81-86] and diarylbibenzofuranone,[87] fluorescence-generating dimers of cinnamates that feature a cyclobutane ring,[88] cyclooctane-containing dimers of anthracene,[89] and maleimide–anthracene cycloadducts[90-92] as well as chemiluminescence-generating bis(adamantyl)-1,2-dioxetanes.[93, 94] Alternatively, blended photoluminescent dyes that form excimers (excited dimers), such as cyano oligo(*p*-phenylene vinylenes) (cyano-OPVs) have been extensively studied.[81-85, 95-97] Other dyes, which include bis(benzoxazolyl) stilbene[98, 99] and perylene derivatives,[100] can be dispersed into polymeric materials during melt compounding or in solution. Further mechanochromic substances that have been used in polymeric materials are shear-responsive photoluminescent ZnO tetrapods,[101] CdSe–CdS tetrapod quantum dots[102] or force-responsive proteins.[103-109] The reader is referred to various reviews for a detailed overview of this field.[6-10]

2.4.2 Mechanochromic coatings and thermoset resins

Most often, mechanochromic substances have been incorporated into thermoplastic polymers, elastomers and other polymer networks, but to a much less extent into fiber-reinforced composites. A reason for this might be that composites deform on a much smaller scale than the other polymer classes when forces are applied because the thermoset resins are brittle and reinforced by fibers. Low strain at break makes it difficult to ensure an effective force transfer from the polymer matrix to the mechanophores. Nevertheless, recently some mechanochromic systems have been specifically developed for epoxy resins and other thermosets that are commonly used as matrices for reinforced composites. Dai's group substituted part of the amine hardener of an epoxy formulation with cinnamamide, the amide of cinnamic acid, which undergoes UV-induced [2 + 2] cycloaddition to its cyclobutane-containing

dimer.[110] In addition, dimers of cinnamamide were directly reacted with an excess of the epoxy monomer, followed by addition of the hardener. When the resulting epoxy resins were compressed, they started to fluoresce due to the cleavage of the cyclobutane ring and recovery of the cinnamoyl moiety. Flinn, Jen and coworkers reacted a dipolar fluorescent dye with bifunctional amines to obtain a nonfluorescent molecule with pendent amine groups, which allowed the covalent incorporation of the mechanophore into an epoxy resin.[111] Compression forces cleaved off the amines, thus regenerating the dipolar dye and turning its fluorescence on. The fluorescence emission intensity increased with compressive strain, so that the materials could be used as built-in strain sensors for composites. The same team discovered that a certain combination of epoxy monomer and amine curing agent (tetraglycidyl-4′-4-diaminodiphenylmethane and diethylenetriamine) results in materials that fluoresce red when compressed. The epoxy thermoset was tested as coating on carbon-fiber-reinforced composites and could report BVID. (**Figure 5**).[112] Most likely, the fluorescence stems from fluorescent radical species that form due to force-induced bond rupture.

Another epoxy resin with mechanochromic properties based on colored radical species was reported by Odriozola and coworkers.[113] 4-Aminophenyl disulfide was used as a hardener for epoxy monomers. Glass fiber-reinforced composites turned green when hit with a hammer. The color disappeared within 24 h. On the molecular scale, the disulfide bond cleaved in response to the applied force, creating sulfenyl radicals. They slowly recombine, causing the color to fade.

Instead of incorporating a mechanophore covalently into the epoxy polymer, it is also possible to blend mechanophore-containing polymers into the epoxy prepolymer before curing. For example, cyclobutane-containing polymers based on cinnamate

derivatives led to materials that started to fluoresce when the material was strained beyond the yield point under compression or when hit with a hammer.[114, 115]

Dai's group reported mechanochromic particles that were completely composed of a mechanophore. Microparticles were formed by dimers of an anthracene dimer that featured a carboxylic acid functional group. They were dispersed into an epoxy resin[116] and a polyurethane thermoset.[117] After curing, the materials were subjected to compression strain, which caused them to become fluorescent. Dimers of anthracene do not fluoresce, while anthracene does. Thus, the results indicate that dimers converted to anthracene monomers in response to the compression. However, it is unclear if the mechanically induced reaction mostly happens at the interface of the particles or throughout the particles.

2.4.2 Mechanophores at the fiber-resin interface

While force-induced activation of chemical bonds in thermoset resins is difficult to achieve because of low strain during deformation of highly crosslinked resins, there is a region in composite materials where forces and local displacements are maximal: the interface between the polymer resin and the reinforcing fibers. Many damage modes lead to interfacial debonding of resin from the surface of fibers because of the mismatch of mechanical properties (elastic modulus, etc.) between the polymer and the fibers. Moreover, cracks propagate through the resin are deflected at these interfaces. Thus, if the mechanophore is not placed in the polymer resin but at the interface between the fibers and the resin, a much more efficient force transduction can be expected. Bruns and coworkers demonstrated this concept by placing fluorescent proteins at the fiber–matrix interface. To this end, enhanced yellow fluorescent protein (eYFP) was covalently immobilized on the surface of glass fibers[106] and of carbon fibers.[107] The fibers where embedded into a transparent

epoxy resin, which formed covalent bonds with the amine groups (and other functional groups) on the surface of the proteins. As a result, the proteins were attached via multiple points to the fiber and the resin. The strategy to first conjugate the proteins onto fibers in aqueous solutions and then embed them into resin elegantly solved the challenge that the water-soluble proteins are immiscible with standard epoxy resins. Fluorescent proteins such as eYFP and green fluorescent protein (GFP) have been discussed for a while as sensors for mechanical forces in biological systems and in materials[118-122] because they lose their fluorescence when their three-dimensional structure is perturbed. Even slight changes to the conformation of the protein disrupt the interactions of the fluorophore within the protein with its surrounding network of hydrogen bonds, hydrophobic interactions and π–π stacking. However, mechanochromic materials based on fluorescent proteins have only been realized recently,[106-109] possibly because the force transfer from the polymer matrix to the relatively large protein is often not efficient enough. In contrast, when placed at the fiber–resin interface, the fluorescence of the proteins readily disappeared when the materials were subjected to low-velocity impacts (**Figure 6**).[106, 107] Regions in which the protein lost its fluorescence where co-located with sites of fiber fracture, but also extended tens of micrometers away from the fracture site, indicating where interfacial debonding happened. Importantly, the presence of the proteins did not reduce the interfacial shear strength of the composites, as demonstrated with single-fiber mechanical tests. It should be noted that proteins, if needed on a large scale, are not as expensive as many material scientists expect. Functional proteins can nowadays be produced biotechnologically as commodities, as is already done, e.g., for enzymes in detergents[123] or for spider silk proteins.[124] Thus, implementation of fluorescent

proteins into composites, at least at selected important points of a composite structure, is a feasible approach to self-reporting materials.

It is much easier to observe the appearance of fluorescence at a site of damage than the disappearance of fluorescence. Thus, systems in which the fluorescence is switched on are highly desirable for self-reporting composites. In this context, Gilman and coworkers used Rhodamine 110 as a mechanophore at the interface of silk fibrils and epoxy resin.[125] The dye was covalently bound to lysine residues of the protein fibers via its carboxylic acid and to the epoxy resin via its amine groups. Upon uniaxial tensile deformation, the spirolactam ring of the molecule opened, which switched the dye from a nonfluorescent to its fluorescent state. Two-photon fluorescence lifetime imaging microscopy revealed that the fluorescence intensity increased with increasing strain and that regions on the silk fibrils differed in their interfacial bond strength to the epoxy resin.

Good mechanical activation of the mechanophore diarylbibenzofuranone at the interface between silica particles and a rubbery poly(butyl acrylate) matrix was recently reported.[126] The composite rubbers changed from colorless to blue when stretched because stable blue radicals formed. In contrast, the same mechanophore did not cause strain-induced coloration in another type of composite.[127] Cellulose nanocrystals were modified with diarylbibenzofuranone and incorporated into a poly(propylene glycol) elastomer that was crosslinked with the same mechanophore. Even though self-healing was observed due to the reversible formation of radicals, the radicals appear to recombine too fast in the soft polymer matrix to develop observable color. These two examples demonstrate that a variety of parameters, such as the type of filler and polymer matrix, their elastic moduli and the properties of the

mechanochromic entities at the interface must match to achieve force-induced colorimetric effects at the interface of composite materials.

The maleimide–anthracene cycloadduct, which liberates fluorescent anthracene in a force-triggered retro-[4 + 2] cycloaddition reaction, was also shown to be more readily activated by mechanical forces at heterointerfaces, albeit so far only at the interface of silica nanoparticles in a solvent[90, 91] or in micelles[92] and not yet in composite materials.

2.4.3 Corrosion detection at the fiber-resin interface

Fluorescent probes at the fiber–polymer interface can also act as sensors for other kinds of damage than those caused by mechanical forces. Seawater leads to a substantial loss in mechanical properties of composites when it penetrates into materials.[26] This is of particular importance for the many fiber-reinforced composites that are intended for use in marine environments, such as in off-shore wind turbines, pipelines, on ships or for parts of bridges. To create a self-reporting material that reports damage by seawater, CdS quantum dots were immobilized on glass fibers and then embedded into an unsaturated isophthalic polyester resin.[128] Immersion of the composites into seawater for months deteriorated the interfacial strength between the fibers and the resin and allowed water to diffuse to the quantum dots and quench their fluorescence. The loss of fluorescence scaled with the loss in tensile strength and flexural strength. In principle, such a system could be used to monitor the material's structural health by fluorescence measurements.

3. Structural health monitoring with embedded sensors

A classical engineering approach to assess the structural integrity of materials is to equip them with sensors, and connect these sensors to data acquisition and processing systems that can be locally or remotely controlled. The analogy in nature would be the nervous system with its receptors as sensing elements, signal transduction via nerves

and signal processing in the brain. For composite materials, the simplest solution is to affix strain gauges onto a structure.[21, 129-131] A strain gauge can be a metal foil pattern on a nonconductive and flexible support. Deformation of the structure changes the resistivity of the conducting layer, which is electronically read out through a Wheatstone bridge. A problem of strain gauges is that they can malfunction, e.g., if the copper wires that connect a gauge with a computer corrode over time[21] or if a structure is hit by lightning, which is a common event in wind turbine rotors. Moreover, they do not efficiently detect delamination within composite plies.[132]

Carbon fibers conduct electricity. Deformation of composites will alter the contact area between fibers and can cause fiber fracture. Thus, electrical resistance measurements can be used to detect damage in carbon fiber-reinforced composites.[133] Alternatively, carbon nanotubes can be added to composites to alter their electrical properties, allowing for structural health monitoring of composites that would otherwise be insulators, such as glass fiber-reinforced composites.[134, 135] Carbon nanotubes can form a percolated three-dimensional network in the resin, whose conductivity will change if microscale damage perturbs it. Conducting networks of carbon nanotubes were also deposited on the surface of nonconductive fibers, allowing measurement of strain and the occurrence of microcracks via the composite's electrical resistance.[136-138] Alternatively, fibers may be spray-coated with carbon nanotubes and embedded as sensing fibers into composites.[139] Such one-dimensional sensors were used to record shrinking during curing and to map strain and stress under load. Thus, similar to the fiber Bragg sensors discussed below, the carbon nanotube-coated fibers allow for lifelong structural health monitoring, from the curing process, through the in-service state until material failure.[140]

Another possibility to measure deformation of materials electronically is to embed piezosensors, so-called piezoelectric microelectromechanical systems (MEMS), into their bulk.[141] Sensors can be an array of piezoceramics as a sensing layer in the composite[17, 142] or they can consist of piezoelectronic materials (such as lead zirconate titanate, barium titanate or aluminum nitride) coated on (hollow) conducting fibers.[143-145]

In contrast to electronic signals, optical signals are not susceptible to electromagnetic interference. Thus, fiber optic sensors have become an important class of sensing elements for structural-health monitoring.[19, 132, 146, 147] The simplest version of a fiber optics sensor is an optical fiber through which light is shone onto a detector. If the fiber breaks, e.g., in cracks of the composite or at sites or BVID, its optical transmission is interrupted, resulting in a modulation of light intensity. It should be noted, however, that optical fibers have a much larger diameter (e.g. 50 or 125 µm)[19] than glass fibers used for reinforcing purposes, so that the reinforcing fibers themselves cannot be used directly as sensing fibers.

More sophisticated fiber optics sensors can detect deformation, e.g., in response to strain. If a good interfacial bonding between fibers and polymer is ensured, the fiber sensors will therefore detect strain of the material and other modes of deformation. Strain measurements can be achieved via interferometric sensors, such as Fabry–Pérot interferometers.[148] More popular are fiber Bragg grating sensors (**Figure 7a**),[19, 132, 146, 147] which also have been used to measure BVID.[149, 150] Here, the refractive index of an optical fiber is modulated in a precise periodic pattern, e.g., by UV interference during production of the sensors. This sensing region acts as a Bragg mirror and reflects defined wavelengths of light that travels through the fiber. As the wavelengths depend on the distance between regions of the same refractive index, i.e., the pitch of

the grating, elongation or compression along the fiber axis will modulate the spectrum of the light that is reflected and of the light that continues to travel along the fiber. Spectral analysis of the light therefore allows measurement of strain in composites.

It is obvious that optical fiber sensors only detect deformation in their vicinity. Thus, they are either placed at critical points of a structure, or a network of sensing elements is embedded into a composite structure to map strain distributions.[146, 151] For the latter, data analysis can become quite complex, and computational methods as well as modeling efforts are employed to correlate strain readings with damage modes and damage locations.[152, 153] In addition, the composite can be probed with ultrasonic waves generated by piezoelectronic transducers and fiber optic strain sensors as receivers, thus allowing to determine the location of damage.[154, 155]

Fiber Bragg grating sensors have already been implemented in large-scale composites. For example, the internal strain in wind turbine blades during stress fatigue tests with more than one million load cycles could be measured by such sensors.[156] In other examples, sensors were placed at strategically selected places on rotor blades which allowed to monitor bending loads during operation of a wind turbine (Figure 7b),[157] or to detect damage.[158, 159] Fiber optic Bragg grating sensors were also used in aeronautic and automotive composite components (Figure 7c).[160] The sensors were embedded into the composites during resin transfer molding. Dynamic strain measurements were used to characterize the vibration properties of the composites. Yet another example describes an array of 40 fiber Bragg grating sensors that was incorporated into an all-fiber reinforced polymer composite road bridge to measure strain in real-time during use of the bridge.[161] Moreover, fiber Bragg grating sensors allow monitoring strain in composites throughout their life cycle, starting from

monitoring strain development during vacuum infusion and curing, to strain under flexural load until materials failure.[162]

An alternative to fiber Bragg grating sensors are fiber-optic sensors that use the Brillouin or Raleigh scattering of light in standard telecom optical fibers.[19, 163, 164] The interrogating monochromatic light travels along the fiber and a small part of it is back scattered by inelastic scattering. The shift in wavelength of the Brillouin scattering depends on the density of the glass, which varies with temperature and strain.[165, 166] The Rayleigh backscattering is caused by fluctuations in refractive index, which also depend on temperature and strain. A defect can be located along the fiber by the time of flight or by phase modulation. As a result, strain (or temperature changes) along the whole length of the fiber are measured with a spatial resolution down to centimeters or lower.[164] Such distributed fiber sensors therefore enable structural health monitoring in large areas of a composite structure. For example, a single optical fiber for Brillouin scattering sensing was embedded into carbon fiber reinforced composite and allowed to measure strain during manufacturing and in impact tests with a spatial resolution of 10 cm.[167] Brillouin-systems were also shown to detect small and large impact traces on a composite pressure vessel.[168] Recent work compared distributed fiber sensors based on Rayleigh scattering with fiber Bragg grating sensors for the sensing of damage in wind turbine blades.[159] Both sensing methods allowed damage detection based on strain measurements and strain field pattern recognition.

4. Discussion and future perspectives

Materials that autonomously sense and report micro-damage, stress or strain can enhance the service life-time of composite components and have the potential to increase the safety of these materials. Moreover, they allow to investigate the build-up of stresses during manufacturing or the propagation of damage under load. This

Progress Report showcases the main approaches that have been followed to achieve self-reporting composite materials. A direct comparison between the various strategies is difficult and there is not one system that is better than all the others. The intrinsic properties of each method define probable application scenarios. The simplest method to render any material self-reporting is to coat it with a damage-indicating coating. The advantage of such bruising coatings is that they usually do not change the mechanical properties of a composite. Moreover, self-reporting of damage via color changes have to be visible on the surface of a material, so that a coating is ideally localized. Types of damage that can be detected by color-changing coatings comprise impacts, indentation, scratches or cuts. However, coatings are less suited for damage detection in response to bending or compression of a material, as the resulting damage often occurs within the composite, e.g. delamination, matrix cracking, fiber fracture, or fiber buckling. Dye-filled microcapsules are the most promising indicators for damage-indicating coatings because they can simply be dispersed into coatings and do not require tailor-made polymers, as it would be the case with mechanophores. Thus, we expect that this technology has a high chance of finding its way into real-world applications.

Microencapsulated damage indicators can outperform natural bruises in terms of longevity of the color signal, as the color of bruises changes with time and then fades away within weeks due to natural healing processes. However, if a bruise disappears, it is a good indication that the damage has healed. Dye-filled capsules are often used in combination with self-healing agents. Very recently, materials have been developed that only transiently reports damage through color changes until the damage has healed.[169, 170] Ideally, the color of the material would also quantify the

state of healing, e.g., by turning from red in case of severe initial damages to orange for intermediate healing states and colorless once completely restored.

Even though dye-filled microcapsules can also be dispersed into the bulk of composites, either into the polymer matrix or immobilized on the surface of reinforcing fibers, dye-filled hollow fibers are the more obvious choice for fiber-reinforced composites, as they can be integrated into or between fiber plies. Vascularized materials are the more sophisticated form of bleeding composites. They allow to deploy crack penetrating dyes (and healing agents) from an external reservoir to damage sites and repeated healing of the same specimen. However, unless the microvascular system is created by stitching sacrificial polymer threats into the reinforcing fiber fabric,[68] microvascular channels are relatively labor-intensive to produce. Many vascular networks rely on capillary forces to draw the liquid into damage sites. This limits the size of addressable damage, because capillary transport is only effective for small cracks. Alternatively, the channels can be interfaced with a pressurized reservoir of dyes and healing agents, or with external dispensers and pumps that require electricity.[171, 172] Thus, they are suitable for applications in which the material performance is critical, but costs are less critical, such as loadbearing components in the aerospace sector. The incorporation of hollow fibers or channels into a composite influences the material´s mechanical properties, such as its fracture toughness or interlaminar shear strength, which has to be taken into account when designing composite laminates and structures.[173, 174] In the context of self-healing materials, hollow fibers and vascular networks work well for damage modes occurring within the material, such as crack growth or delamination of plies. However, for a visual self-reporting effect, either both the polymer matrix and the reinforcing fibers have to be transparent, or the dye that is released into the damage has to

penetrate through cracks up to the surface of the material. The latter is of course only possible if cracks reach the surface. Bending can lead to cracks or delaminated zones that extend from the bulk of a composite to its surface. Moreover, BVID extends from the surface into the material and can therefore be detected on the surface by bleeding of dyes.

Mechanophores, mechanochromic aggregates and force-responsive proteins remain at the site of damage. Therefore, whether they are embedded in the polymer matrix or located at the fiber-resin interface, their color or fluorescence changes will only be visible in the topmost layer of a laminate, unless the whole composite is transparent. This notion is of particular relevance in carbon fiber reinforced composites because the black carbon fibers hinder optical assessment of the interior of a composite. Therefore, mechanochromic self-reporting of damage with these systems is mostly suitable to detect BVID. From these considerations, it is also obvious that only the fiber ply closest to a surface or the topmost layer of resin has to be equipped with mechano-responsive molecules, which can greatly reduce the costs of such self-reporting materials. A clear advantage of these molecular stress and strain sensing elements over microscopic capsules or channels is that they have the potential to detect damage and deformation at the molecular level, which makes them very interesting analytical tools to study crack growth, interfacial debonding or matrix deformation. This feature permits to improve our understanding of damage evolution in composites on the nanoscale. However, while threshold forces for the activation of some mechanophores have been measured by single molecule force spectroscopy,[119, 120, 175] the potential of mechanochromic molecular systems has not been exploited to systematically study damage propagation on the nanoscale in composite materials.

Electronic or optical sensing elements such as strain gauges, fiber optics sensors or resistance measurements, are the most mature approach towards self-reporting materials. They allow measuring the build-up of internal stresses during composite production, strain in service, BVID and other damage types. With a detailed knowledge of the material's response to deformation, the data can be used to monitor the structural health of the materials. The individual methods have their strengths and weaknesses. For example, advantages of fiber Bragg grating sensors are their high sensitivity, low power consumption, small size, low weight and that their signal is not affected by electromagnetic interference.[152] However, they do not only measure strain due to mechanical forces. Their signal is also modulated by temperature effects, such as thermal expansion and changes in refractive index. These thermal effects need to be compensated during strain measurements in real operational scenarios.[159] Distributed optical fiber sensors based on Brillouin scattering can measure strain with high precision and high spatial resolution. Importantly, they can replace many point sensors because the whole length of the optical fiber acts as sensor. The effect of temperature on the signal during strain measurements has to be taken into account also with this type of sensors. However, Brillouin scattering-based fiber optic sensors offer the possibility to measure strain and temperature with the same fiber, e.g. by shielding part of it from strain while the rest of the fiber measures the combined effect of strain and temperature.[176] Alternatively, two fibers can be used, one of which is isolated from mechanical strain.[177] A detailed comparison of the characteristics of various electronic, optical, and acoustic sensing technologies is beyond the scope of this article and the reader is referred to some excellent reviews and books.[19, 27, 164, 178] A disadvantage of all classic sensing approaches is that they require additional data acquisition equipment nearby the composite component, which adds weight and

which has to be implemented into the design of composite structures. In comparison, color- or fluorescence-changing materials would, in an ideal case, only need visual or photographic inspection to detect damage sites. Nevertheless, extrinsic or intrinsic sensors will remain the state-of-the art for structural health monitoring for the foreseeable future, because they are based on existing and well-developed technologies. Moreover, many sensor systems for structural health monitoring are commercially available.

It should be noted that only the mature engineering approaches toward self-sensing, such as optical fiber sensors and resistance sensors, have been implemented and tested on a large scale, e.g., in aircraft composite structures,[19] in wind turbine blades,[20, 21, 159] or in civil infrastructure.[26] In contrast, mechanochromic systems, whether based on capsules, hollow fibers, vascular systems, mechanophores, dye aggregates or biomolecules, have only been investigated in research and development laboratories. While this allows for excellent science and enables the creative design of new self-reporting principles, their industrial implementation faces several challenges that need to be addressed in future research. For example, threshold stresses are unknown for most mechanochromic materials, but are required to evaluate the ability of materials to reliable report damage-relevant stress levels. One of the few examples in which threshold forces were determined for self-reporting composites are the leuco-dye-filled microcapsules that have been immobilized on reinforcing nylon fibers (*vide supra*).[36] The threshold stress at which the capsules start to collapse and release their content was 77 MPa, which is the same order of magnitude than the strength of the epoxy binder. Ideally, self-reporting materials would not only show an on/off response, but respond with a gradual change in color or fluorescence intensity in response to increasing load. Such systems are only starting to emerge in literature.

Figure 5 shows the gradual increase in optical signal intensity of a mechanochromic epoxy resin as a function of increasing compressive stress.[112] The fluorescence threshold is at ~1.0 GPa. Another recent example, albeit not for composites but for poly(dimethylsoloxane) rubbers, are microencapsulated excimer-forming dyes that were used to prepare materials with a ratiometric response to mechanical deformation and impact.[179]

Very important for a reliable assessment of damage is to avoid false-positive and false-negative results. False-positive signals would lead to unnecessary repairs, but false negative results would severely impede the safety of the structure, as the user would not be warned about potential hazardous damage. Thus, it has to be ensured that the sensing elements are failure safe. Unfortunately, statistical evaluation of the failure rate of self-reporting mechanochromic composites has not yet been addressed in the scientific literature. Evaluation of false negative results goes hand-in-hand with the stability of the self-reporting mechanisms. The employed systems must be stable in-use for extended time, often for years, withstanding UV irradiation, heat and cold, and even corrosive environments.

In order to implement self-reporting color-changing composites in real-world applications, devices need to be developed to read out, quantify and document color and fluorescence signals on large surfaces. For example, climbing robots that have been designed for the nondestructive evaluation of wind blades[180] or other automated scanning devices[2] could be equipped with cameras or fluorescence sensors.

Other major issues to overcome are the scalability of the production of mechanochromic indicators, and especially the costs that are associated with these tailor-made functional molecules. To reduce the amount of sophisticated mechanophores needed and therefore to keep the costs of self-reporting composites

reasonable, mechanophore-equipped fibers might only be added as safety threads into the topmost layer of a laminate, and self-reporting capabilities could be limited to neuralgic points of a structure. Another very important aspect to consider is that many composite materials need to be certified by the authorities for their intended use, especially in the aerospace sector. This requirement limits the possibility to introduce novel chemistries and additives to real-world materials and delays the transfer of innovation from materials research labs into industrial application.

5. Conclusion

The reviewed work demonstrates that self-reporting composites are possible and that failure of the polymer matrix, interfacial defects, delamination and fiber fracture can be visualized by color or fluorescence changes or detected by electronic or optical probes within the material. Many of the concepts are inspired by the way living organisms sense and detect stress and damage, and are often combined with self-healing capabilities. Self-reporting materials allow detection of micron-scale damage within the composites, such as BVID caused by low-velocity impacts, and therefore enable structural health monitoring of composite parts while they are in use or during maintenance inspections. As small damage sites can grow under load, self-reporting materials can increase the safety of composite materials and potentially prevent accidents. Moreover, these approaches allow increasing service intervals or a decrease in the amount of material needed, thus making composite structures more cost efficient and lightweight.

The biological world with its many wonders on the macroscopic and molecular scale will continue to serve as source of inspiration for novel stimuli-responsive materials and we are convinced that many exciting new concepts for self-reporting materials will emerge in the near future. However, to achieve feasible self-reporting composites for practical applications, materials scientists will have to work hand in hand with

engineers and intensify their efforts to address the challenges mentioned in the previous chapter, such as scalability, stability, and endurance to environmental stresses.

Corresponding author:

Nico Bruns is Associate Professor of Macromolecular Chemistry at the Adolphe Merkle Institute of the University of Fribourg, Switzerland. He obtained his PhD in Polymer Chemistry from the University of Freiburg (Germany), was a Postdoc in Biotechnology at the University of California, Berkeley and started 2008 his independent academic career at the University of Basel. In 2013, he received a prestigious Swiss National Science Foundation Professorship, which allowed him to take up his current position. His research interest is bio-inspired polymer chemistry, in particular force-responsive polymer-protein materials, biocatalytic nanoreactors and enzyme catalyzed ATRP (bioATRP).

TOC:
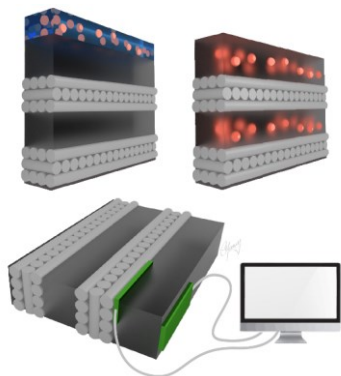
Living beings are able to sense strain and damage to their tissue and can therefore avoid long lasting damage, or protect and heal the damaged part of the body. Self-reporting fiber-reinforced composites are reviewed that mimic these phenomena, e.g. by force-induced color changes, by vascular bleeding, or by electronic and fiber optic sensing elements.

Figures and Tables:
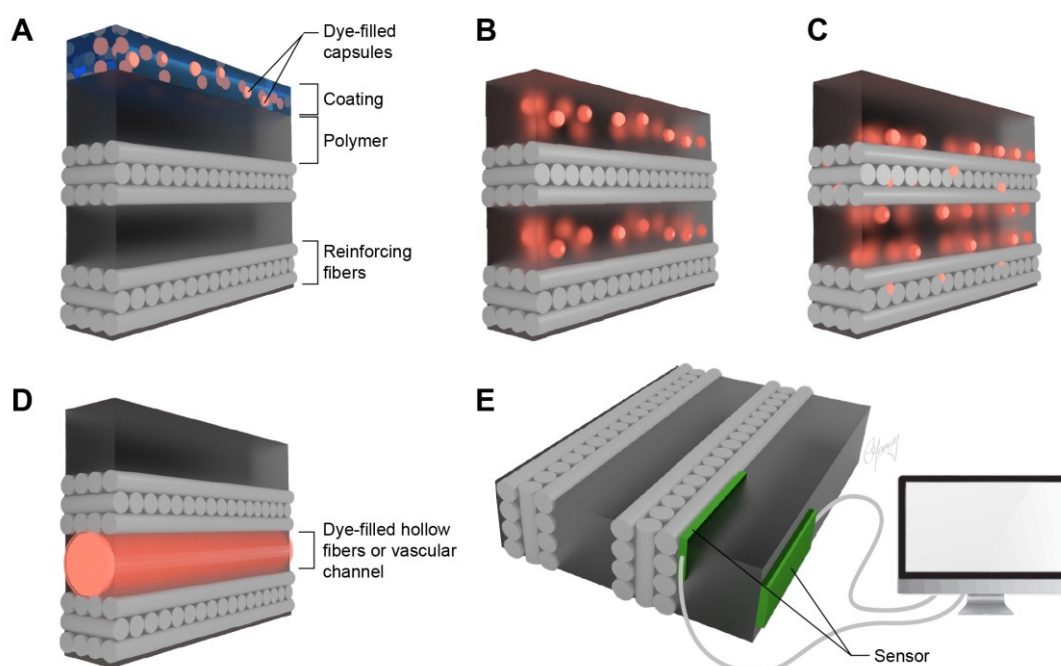
Figure 1. Approaches to self-reporting fiber-reinforced composites. In analogy to the formation of bruises and bleeding wounds, optical cues can indicate deformation and damage. Such changes in color, fluorescence or luminescence can be achieved by damage-indicating coatings (**A**), and by dye-filled microcapsules or mechanochromes that are dispersed into the polymer matrix (**B**) or that are bound onto the surface of the reinforcing fibers (**C**). Alternatively, dye-filled hollow fibers or vascular microchannels can be integrated into composites (**D**). Sensing of damage to tissue by nerve signals can be mimicked via electrical or optical sensors that are attached onto or integrated into composites structures (**E**).

Figure 2. Self-reporting coating with high contrast between damaged and undamaged areas based on dye-filled microcapsules. A. Conceptual scheme of release of an almost colorless dye from capsules into damaged areas, where it encounters basic amine groups of the polymer resin and develops color. **B**. pH-dependent color changes of 2′,7′-dichlorofluorescein, the dye that was used to achieve the self-reporting effect. **C**. Photograph of a coating that has developed red color in a scratch. **D**. Microscopy image of a scratch in the self-reporting coating, showing color-changed microcapsules in the vicinity of the damage. Reproduced with permission from Ref. [37]. Copyright 2016, Wiley-VCH Verlag GmbH & Co. KGaA.
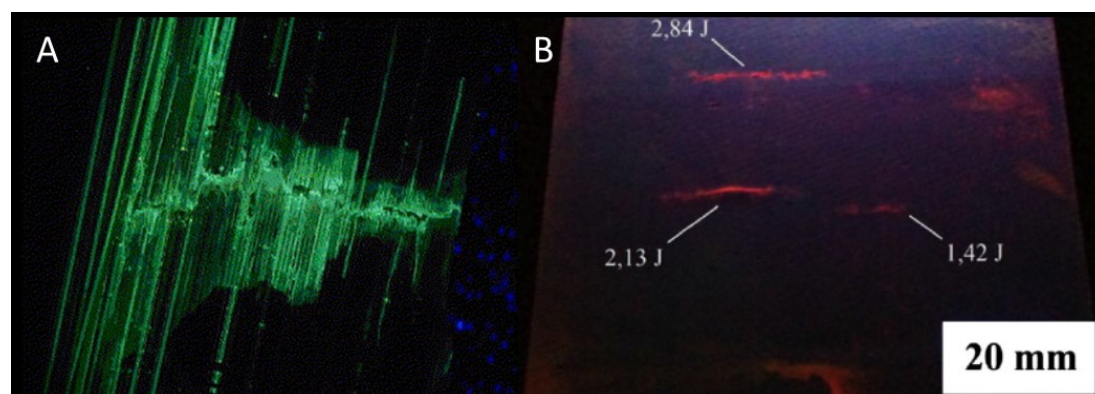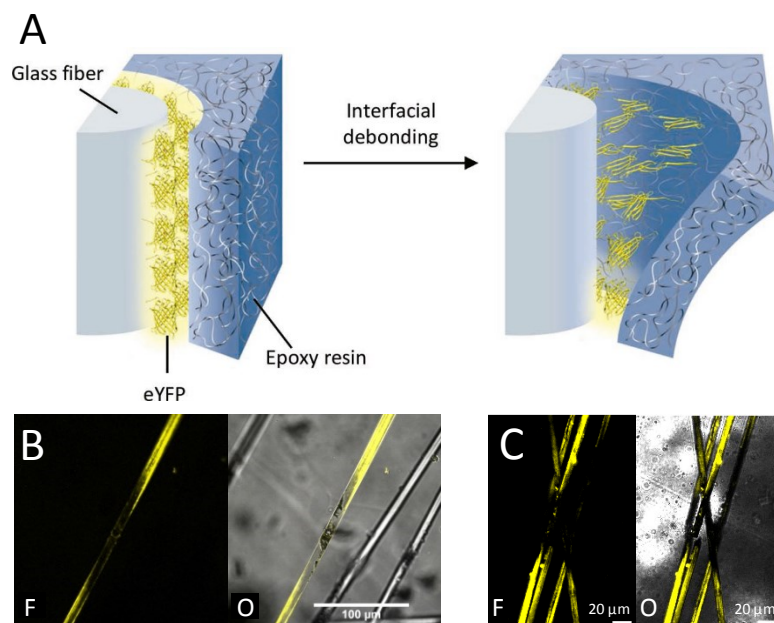

Figure 3. **Self-reporting fiber-reinforced composites based on fluorescent dyes that bleed out of hollow glass fibers. A**. Fluorescent microscopy image of a bleeding composite (45x magnification). Flexural bending resulted in fracture, and the dye allows to visualize the extend and the location of this damage. **B**. Photograph of an UV-illuminated self-reporting composite after impacts, showing damage on the backside of the sample. Reproduced with permission from Refs. [47] and [51]. Copyright 2005 and 2014, Elsevier.
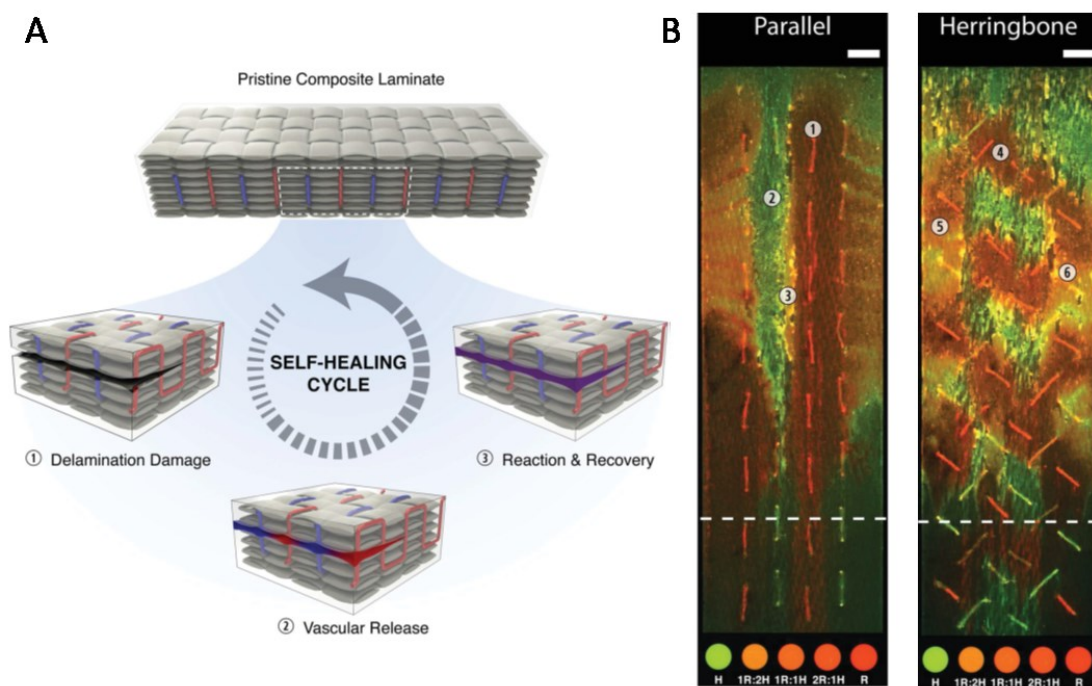
Figure 4. Vascularized self-healing and self-reporting glass fiber-reinforced epoxy composites. A. Schematic representation of a composite into which vascular channels have been incorporated by stitching of PLA fibers into glass fiber fabrics, followed by vaporization of the sacrificial PLA. The resulting channels were filled with two liquid components of a healing reagent. Each component was stained with a fluorescent dye. Upon delamination of fiber plies, the channels ruptured and released the healing agents into the damaged zone. Where the they met, they polymerized and restored structural integrity. **B**. Fluorescence photography images of vascularized specimen after delamination damage and self-healing. The two fluorescent dyes visualize the distribution and mixing of healing agents in the damaged zones. Numbers highlight areas of different mixing ratios according to the color scale beneath the images. The targeted mixing ratio of 2R:1H appears dark orange and is achieved, e.g. at location 5. (H = triethylenetetramine based hardener; R = diglycidyl ether of bisphenol A based epoxy resin; scale bars: 5 mm) Adapted with permission from Ref. [66]. Copyright 2014, Wiley-VCH Verlag GmbH & Co. KGaA.
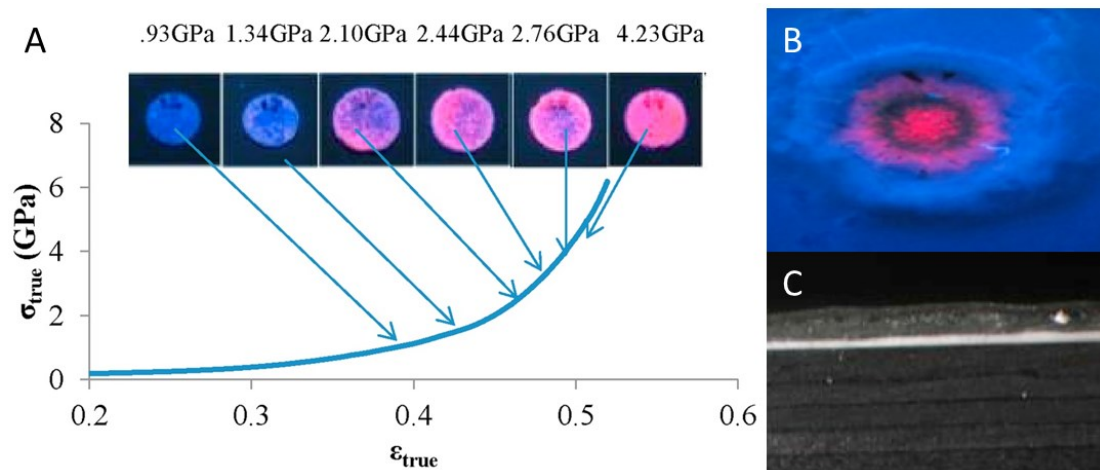
Figure 5. Mechanochromic epoxy coating to detect barely visible impact damage (BVID) in carbon fiber-reinforced composites. A. Stress–strain compression curve of mechanochromic epoxy resin and fluorescence images of sample discs after compression. The force-induced fluorescence of the specimen increases with the applied stress. **B**. Fluorescence image (top-view) of an impacted composite that is coated with the mechanochromic epoxy coating. The coating self-reported BVID. **C**. Cross-section of the coated composite, showing plies of carbon fibers, the mechanochromic epoxy coating (in light gray) and a clear polyurethane topcoat. Reproduced with permission from Ref. [112]. Copyright 2017, Elsevier.

Figure 6. Yellow fluorescent protein as a mechanophore for self-reporting fiber-reinforced composites. A. Schematic representation of debonding between the epoxy resin and the glass fiber, forcing the fluorescent protein to unfold and to lose its fluorescence. (Size of fiber and protein not to scale.) **B**. Confocal fluorescence microscopy image of eYFP-coated glass fibers in an epoxy resin after low velocity impact. **C**. Z-stack projection of confocal fluorescence microscopy images of eYFP-coated carbon fibers in an epoxy resin after low velocity impact. The loss of fluorescence in the microscopy images indicates regions of interfacial debonding around sites of fiber fracture. (F: yellow fluorescence channel; O: overlay of fluorescence and transmission images) Adapted with permission from Refs. [106] and [107]. Copyright 2013, Wiley-VCH Verlag GmbH & Co. KGaA, and copyright 2014, Royal Society of Chemistry.
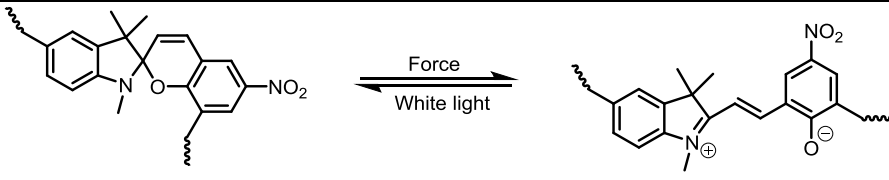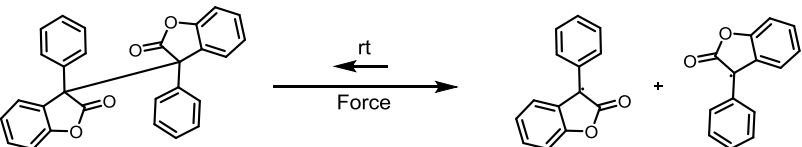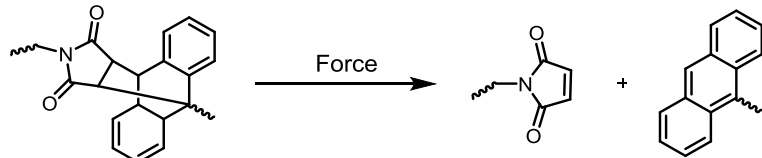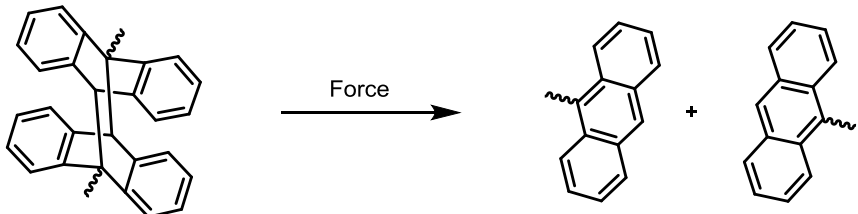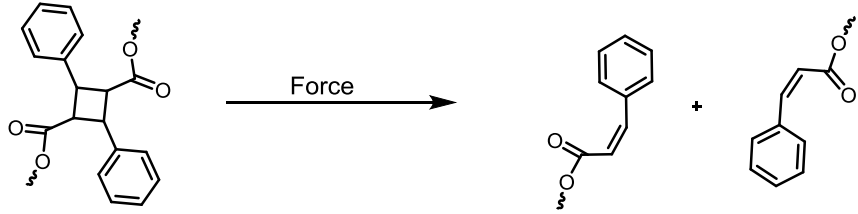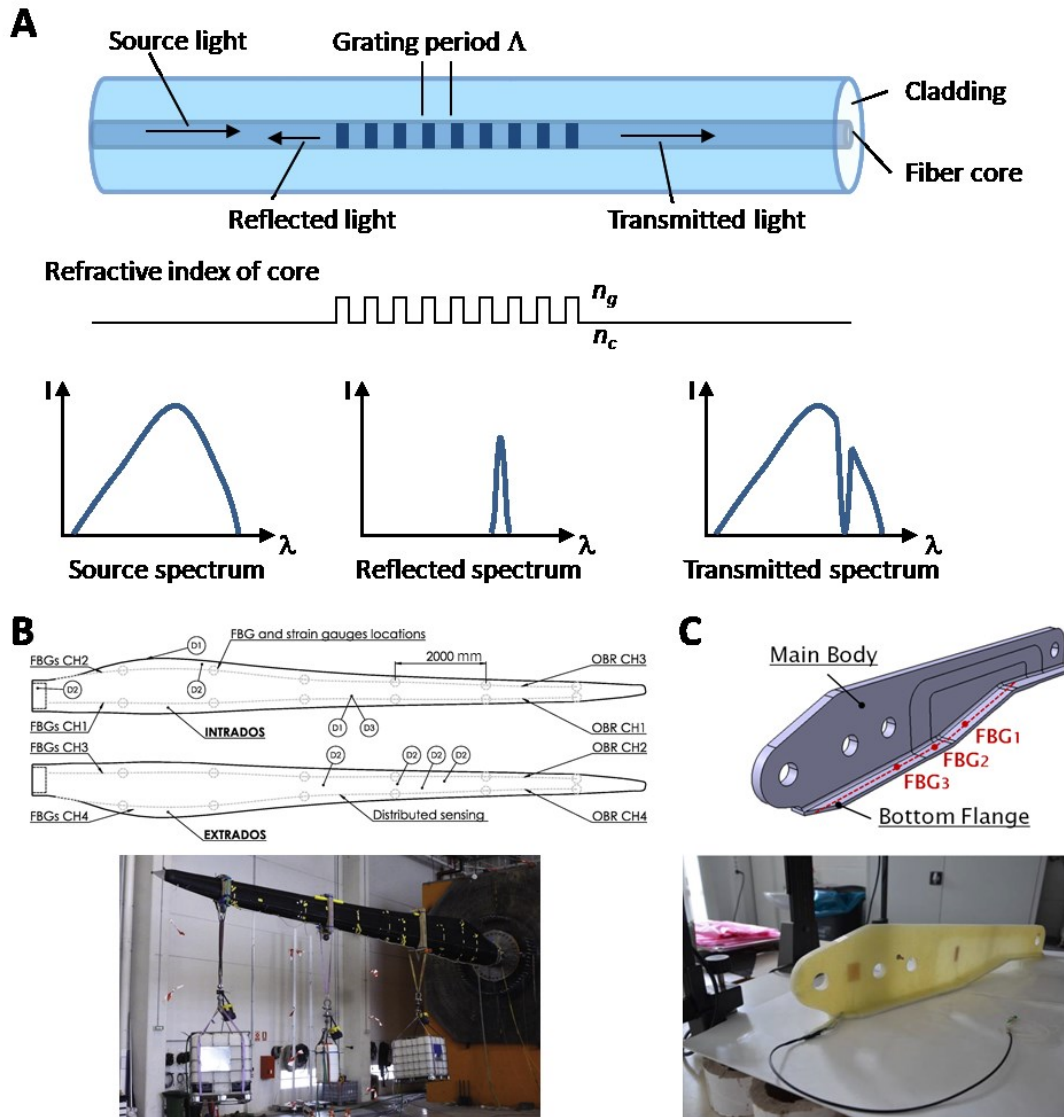
Figure 7. Fiber Bragg grating optical sensors for structural health monitoring in composites. A. Working principal of a fiber Bragg grating sensor. The refractive index of an optical fiber is modulated in defined distances. Light travels through the fiber, some wavelengths are reflected by this Bragg mirror while all other wavelengths continue to travel through the fiber. The reflected and the transmitted spectrum change if the fiber sensor is strained because the pitch of the Bragg mirror changes. **B**. Example for the position of fiber Bragg grating sensors (FBGs), fiber optics for distributed sensing via optical backscatter reflectometer (OBR), and conventional strain gauges distributed in and on the blade of a wind turbine to measure damage locations (D1 etc.). Photography of an experimental setup to apply load at different points of the blade in order to emulate the load distribution during operation. **C.** Schematic design and photography of a glass-fiber-reinforced aeronautic hinge arm with three embedded fiber Bragg sensors for vibration measurements. B) adapted with permission from Ref. [159]. Copyright 2016, Elsevier; C) adapted under the terms of Creative Commons Attribution License CC BY 4.0 from Ref. [160].

Table 1. Common mechanophores and their mechanisms of force-induced color, fluorescence or luminescence changes.

Entry	Mechanophore	Force-induced chemical transformation
1	Spiropyran	
2	Diaryldibenzofuranone	
3	Anthracene–Maleimide cycloadducts	
4	Dimers of anthracene (with cyclooctane ring)	
5	Cinnamate dimers (with cyclobutane ring)	

6	Bis(adamantyl)-1,2-dioxetane	
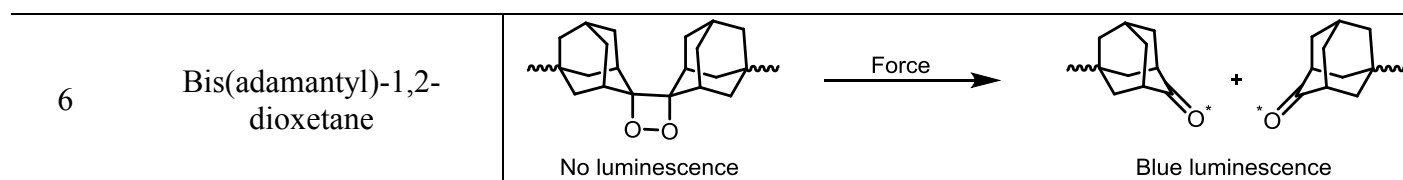
[1]   I. Amenabar, A. Mendikute, A. López-Arraiza, M. Lizaranzu, J. Aurrekoetxea, *Compos. Part B: Eng.* **2011**, *42*, 1298.

[2]   R. Yang, Y. He, H. Zhang, *Renewable Sustainable Energy Rev.* **2016**, *60*, 1225.

[3]   X. E. Gros, in *Handbook of polymer testing: physical methods*, (Ed: R. Brown), Marcel Dekker, New York 1999, 773-840.

[4]   M. O. W. Richardson, M. J. Wisheart, *Compos. Part A: Appl. Sci. Manufact.* **1996**, *27*, 1123.

[5]   U. Polimeno, M. Meo, *Compos. Struct.* **2009**, *91*, 398.

[6]   M. M. Caruso, D. A. Davis, Q. Shen, S. A. Odom, N. R. Sottos, S. R. White, J. S. Moore, *Chem. Rev.* **2009**, *109*, 5755.

[7]   A. L. Black, J. M. Lenhardt, S. L. Craig, *J. Mater. Chem.* **2011**, *21*, 1655.

[8]   J. F. Patrick, M. J. Robb, N. R. Sottos, J. S. Moore, S. R. White, *Nature* **2016**, *540*, 363.

[9]   J. V. Araujo, O. Rifaie-Graham, E. A. Apebende, N. Bruns, in *Bio-inspired Polymers, RSC Polymer Chemistry Series No. 22*, (Eds: N. Bruns, A. F. M. Kilbinger), The Royal Society of Chemistry, Cambridge, UK 2017, 354-401.

[10]   C. Calvino, L. Neumann, C. Weder, S. Schrettl, *J. Polym. Sci., Part A: Polym. Chem.* **2017**, *55*, 640.

[11]   M. D. Hager, P. Greil, C. Leyens, d. Z. S. van, U. S. Schubert, *Adv. Mater. (Weinheim, Ger.)* **2010**, *22*, 5424.

[12]   B. J. Blaiszik, S. L. B. Kramer, S. C. Olugebefola, J. S. Moore, N. R. Sottos, S. R. White, *Annu. Rev. Mater. Res.* **2010**, *40*, 179.

[13]   D. Y. Zhu, M. Z. Rong, M. Q. Zhang, *Prog. Polym. Sci.* **2015**, *49–50*, 175.

[14]   C. E. Diesendruck, N. R. Sottos, J. S. Moore, S. R. White, *Angew. Chem., Int. Ed.* **2015**, *54*, 10428.

[15]   M. Scheiner, T. J. Dickens, O. Okoli, *Polymer* **2016**, *83*, 260.

[16]   K. K. Chawla, *Composite Materials: Science and Engineering*, Springer Science & Business Media, New York, USA 2012.

[17]   L. Ye, Y. Lu, Z. Su, G. Meng, *Compos. Sci. Technol.* **2005**, *65*, 1436.

[18]   Y. Liu, H. Du, L. Liu, J. Leng, *Smart Mater. Struct.* **2014**, *23*, 023001.

[19]   R. Di Sante, *Sensors* **2015**, *15*, 18666.

[20]   C. C. Ciang, J.-R. Lee, H.-J. Bang, *Meas. Sci. Technol.* **2008**, *19*, 122001.

[21]   D. Li, S.-C. M. Ho, G. Song, L. Ren, H. Li, *Smart Mater. Struct.* **2015**, *24*, 033001.

[22]   K. Friedrich, A. A. Almajid, *Appl. Compos. Mater.* **2013**, *20*, 107.

[23]   B. E. Spencer, in *Handbook of Composites*, (Ed: S. T. Peters), Springer US, Boston, MA 1998, 1044-1052.

[24]   M. S. Scholz, J. P. Blanchfield, L. D. Bloom, B. H. Coburn, M. Elkington, J. D. Fuller, M. E. Gilbert, S. A. Muflahi, M. F. Pernice, S. I. Rae, J. A. Trevarthen, S. C. White, P. M. Weaver, I. P. Bond, *Compos. Sci. Technol.* **2011**, *71*, 1791.

[25]   C. E. Bakis, L. C. Bank, V. L. Brown, E. Cosenza, J. F. Davalos, J. J. Lesko, A. Machida, S. H. Rizkalla, T. C. Triantafillou, *J. Compos. Constr.* **2002**, *6*, 73.

[26]   L. C. Hollaway, *Constr. Build. Mater.* **2010**, *24*, 2419.

[27]   D. Balageas, C.-P. Fritzen, A. Güemes, *Structural Health Monitoring*, Wiley-ISTE, London, UK 2006.

[28]   C. R. Farrar, K. Worden, *Philos. Trans. R. Soc., A* **2007**, *365*, 303.

[29]   J. A. Epaarachchi, G. C. Kahandawa, *Structural Health Monitoring Technologies and Next-Generation Smart Composite Structures*, CRC Press, Boca Raton, FL, USA 2016.

[30]   B. E. Koene, M. E. Rogers, *USA Patent WO2006105290 A3*, 2006.

[31]   Air Force SBIR Program: Impact Indicator Paint for Composites, http://www.afsbirsttr.com/Publications/Documents/Innovation-091908-Luna-AF04-133.pdf, accessed: 02/2016,

[32]   L. Monier, K. Jeune, I. Kondolff, G. Vilaça, in *Smart Intelligent Aircraft Structures (SARISTU): Proceedings of the Final Project Conference*, (Eds: C. P. Wölcken, M. Papadopoulos), Springer International Publishing, Cham 2016, 735-743.

[33]   S. R. White, N. R. Sottos, P. H. Geubelle, J. S. Moore, M. R. Kessler, S. R. Sriram, E. N. Brown, S. Viswanathan, *Nature (London, U. K.)* **2001**, *409*, 794.

[34]   M. A. White, *J. Chem. Edu.* **1998**, *75*, 1119.

[35]   S. Vidinejevs, A. N. Aniskevich, A. Gregor, M. Sjöberg, G. Alvarez, *J. Intell. Mater. Syst. Struct.* **2012**, *23*, 1371.

[36]   S. Vidinejevs, O. Strekalova, A. Aniskevich, S. Gaidukov, *Mech. Compos. Mater.* **2013**, *49*, 77.

[37]   W. Li, C. C. Matthews, K. Yang, M. T. Odarczenko, S. R. White, N. R. Sottos, *Adv. Mater. (Weinheim, Ger.)* **2016**.

[38]   S. A. Odom, A. C. Jackson, A. M. Prokup, S. Chayanupatkul, N. R. Sottos, S. R. White, J. S. Moore, *ACS Appl. Mater. Interfaces* **2011**, *3*, 4547.

[39]   B. Di Credico, G. Griffini, M. Levi, S. Turri, *ACS Appl. Mater. Interfaces* **2013**, *5*, 6628.

[40]   M. J. Robb, W. Li, R. C. R. Gergely, C. C. Matthews, S. R. White, N. R. Sottos, J. S. Moore, *ACS Cent. Sci.* **2016**, *2*, 598.

[41]   Y. K. Song, B. Kim, T. H. Lee, J. C. Kim, J. H. Nam, S. M. Noh, Y. I. Park, *Macromol. Rapid Commun.* **2017**, *38*, 1600657.

[42]   G. Postiglione, A. Colombo, C. Dragonetti, M. Levi, S. Turri, G. Griffini, *Sens. Actuators, B* **2017**, *248*, 35.

[43]   A. Lavrenova, J. Farkas, C. Weder, Y. C. Simon, *ACS Appl. Mater. Interfaces* **2015**, *7*, 21828.

[44]   B. J. Blaiszik, M. Baginska, S. R. White, N. R. Sottos, *Adv. Funct. Mater.* **2010**, *20*, 3547.

[45]   C. Dry, *Compos. Struct.* **1996**, *35*, 263.

[46]   S. M. Bleay, C. B. Loader, V. J. Hawyes, L. Humberstone, P. T. Curtis, *Compos. Part A: Appl. Sci. Manufact.* **2001**, *32*, 1767.

[47]   J. W. C. Pang, I. P. Bond, *Compos. Part A: Appl. Sci. Manufact.* **2005**, *36*, 183.

[48]   J. W. C. Pang, I. P. Bond, *Compos. Sci. Technol.* **2005**, *65*, 1791.

[49]   S. Zainuddin, T. Arefin, A. Fahim, M. V. Hosur, J. D. Tyson, A. Kumar, J. Trovillion, S. Jeelani, *Compos. Struct.* **2014**, *108*, 277.

[50]   Y. K. Guo, L. Chen, D. G. Xu, J. R. Zhong, G. Z. Yue, D. Astruc, M. B. Shuai, P. X. Zhao, *RSC Adv.* **2016**, *6*, 65067.

[51]   S. Kling, T. Czigány, *Compos. Sci. Technol.* **2014**, *99*, 82.

[52]   C. J. Norris, G. J. Meadway, M. J. O'Sullivan, I. P. Bond, R. S. Trask, *Adv. Funct. Mater.* **2011**, *21*, 3624.

[53]   R. Shmulsky, P. D. Jones, in *Forest Products and Wood Science An Introduction*, Wiley-Blackwell, 2011, 65-78.

[54]   K. Kuroda, K. Shimaji, *For. Sci.* **1983**, *29*, 653.

[55]   P. R. Larson, *The vascular cambium: development and structure*, Springer Science & Business Media, 2012.

[56]   C. J. Hansen, W. Wu, K. S. Toohey, N. R. Sottos, S. R. White, J. A. Lewis, *Adv. Mater. (Weinheim, Ger.)* **2009**, *21*, 4143.

[57]   K. S. Toohey, N. R. Sottos, J. A. Lewis, J. S. Moore, S. R. White, *Nat. Mater.* **2007**, *6*, 581.

[58]   C. J. Norris, I. P. Bond, R. S. Trask, *Compos. Part A: Appl. Sci. Manufact.* **2011**, *42*, 639.

[59]   C. Gualandi, A. Zucchelli, M. Fernández Osorio, J. Belcari, M. L. Focarete, *Nano Lett.* **2013**, *13*, 5385.

[60]   G. Postiglione, M. Alberini, S. Leigh, M. Levi, S. Turri, *ACS Appl. Mater. Interfaces* **2017**, *9*, 14371.

[61]   F. Omosola, R. Kevin, B. Biswajit, *Smart Mater. Struct.* **2014**, *23*, 095017.

[62]   C.-Y. Huang, R. S. Trask, I. P. Bond, *J. R. Soc. Interface* **2010**, *7*, 1229.

[63]   C. J. Norris, I. P. Bond, R. S. Trask, *Compos. Part A: Appl. Sci. Manufact.* **2013**, *44*, 78.

[64]   T. S. Coope, D. F. Wass, R. S. Trask, I. P. Bond, *Smart Mater. Struct.* **2014**, *23*, 115002.

[65]   R. Luterbacher, R. S. Trask, I. P. Bond, *Smart Mater. Struct.* **2016**, *25*, 015003.

[66]   J. F. Patrick, K. R. Hart, B. P. Krull, C. E. Diesendruck, J. S. Moore, S. R. White, N. R. Sottos, *Adv. Mater. (Weinheim, Ger.)* **2014**, *26*, 4302.

[67]   J. F. Patrick, B. P. Krull, M. Garg, C. L. Mangun, J. S. Moore, N. R. Sottos, S. R. White, *Compos. Part A: Appl. Sci. Manufact.* **2017**, *100*, 361.

[68]   A. P. Esser-Kahn, P. R. Thakre, H. Dong, J. F. Patrick, V. K. Vlasko-Vlasov, N. R. Sottos, J. S. Moore, S. R. White, *Adv. Mater. (Weinheim, Ger.)* **2011**, *23*, 3654.

[69]   R. Klajn, *Chem. Soc. Rev.* **2014**, *43*, 148.

[70]   D. A. Davis, A. Hamilton, J. Yang, L. D. Cremar, D. Van Gough, S. L. Potisek, M. T. Ong, P. V. Braun, T. J. Martínez, S. R. White, *Nature* **2009**, *459*, 68.

[71]   M. Li, Q. Zhang, S. Zhu, *Polymer* **2016**, *99*, 521.

[72]   G. R. Gossweiler, C. L. Brown, G. B. Hewage, E. Sapiro-Gheiler, W. J. Trautman, G. W. Welshofer, S. L. Craig, *ACS Appl. Mater. Interfaces* **2015**, *7*, 22431.

[73]   G. R. Gossweiler, G. B. Hewage, G. Soriano, Q. Wang, G. W. Welshofer, X. Zhao, S. L. Craig, *ACS Macro Lett.* **2014**, *3*, 216.

[74]   Q. Wang, G. R. Gossweiler, S. L. Craig, X. Zhao, *Nat. Commun.* **2014**, *5*, 4899.

[75]   A.-D. N. Celestine, B. A. Beiermann, P. A. May, J. S. Moore, N. R. Sottos, S. R. White, *Polymer* **2014**, *55*, 4164.

[76]   C. M. Kingsbury, P. A. May, D. A. Davis, S. R. White, J. S. Moore, N. R. Sottos, *J. Mater. Chem.* **2011**, *21*, 8381.

[77]   M. E. Grady, B. A. Beiermann, J. S. Moore, N. R. Sottos, *ACS Appl. Mater. Interfaces* **2014**, *6*, 5350.

[78]   G. Hong, H. Zhang, Y. Lin, Y. Chen, Y. Xu, W. Weng, H. Xia, *Macromolecules* **2013**, *46*, 8649.

[79]   Y. Chen, H. Zhang, X. Fang, Y. Lin, Y. Xu, W. Weng, *ACS Macro Lett.* **2014**, *3*, 141.

[80] G. I. Peterson, M. B. Larsen, M. A. Ganter, D. W. Storti, A. J. Boydston, *ACS Appl. Mater. Interfaces* **2014**, *7*, 577.

[81] C. Löwe, C. Weder, *Adv. Mater. (Weinheim, Ger.)* **2002**, *14*, 1625.

[82] B. R. Crenshaw, C. Weder, *Chem. Mater.* **2003**, *15*, 4717.

[83] B. R. Crenshaw, C. Weder, *Adv. Mater. (Weinheim, Ger.)* **2005**, *17*, 1471.

[84] B. R. Crenshaw, C. Weder, *Macromolecules* **2006**, *39*, 9581.

[85] A. Lavrenova, A. Holtz, Y. C. Simon, C. Weder, *Macromol. Mater. Eng.* **2016**.

[86] A. Lavrenova, D. W. Balkenende, Y. Sagara, S. Schrettl, Y. C. Simon, C. Weder, *J. Am. Chem. Soc.* **2017**, *139*, 4302.

[87] K. Imato, A. Irie, T. Kosuge, T. Ohishi, M. Nishihara, A. Takahara, H. Otsuka, *Angew. Chem., Int. Ed.* **2015**, *54*, 6168.

[88] S.-Y. Cho, J.-G. Kim, C.-M. Chung, *Sens. Actuators, B* **2008**, *134*, 822.

[89] Y.-K. Song, K.-H. Lee, W.-S. Hong, S.-Y. Cho, H.-C. Yu, C.-M. Chung, *J. Mater. Chem.* **2012**, *22*, 1380.

[90] J. Li, T. Shiraki, B. Hu, R. A. E. Wright, B. Zhao, J. S. Moore, *J. Am. Chem. Soc.* **2014**, *136*, 15925.

[91] J. Li, B. Hu, K. Yang, B. Zhao, J. S. Moore, *ACS Macro Lett.* **2016**, *5*, 819.

[92] H. Li, Y. Zhang, Y. Liu, R. P. Sijbesma, J. P. A. Heuts, Q. Zhang, *Polym. Chem.* **2017**, *8*, 3971.

[93] Y. Chen, A. J. H. Spiering, S. Karthikeyan, G. W. M. Peters, E. W. Meijer, R. P. Sijbesma, *Nat. Chem.* **2012**, *4*, 559.

[94] E. Ducrot, Y. Chen, M. Bulters, R. P. Sijbesma, C. Creton, *Science* **2014**, *344*, 186.

[95] C. Löwe, C. Weder, *Synthesis* **2002**, *2002*, 1185.

[96] M. Kinami, B. R. Crenshaw, C. Weder, *Chem. Mater.* **2006**, *18*, 946.

[97] J. Lott, C. Weder, *Macromol. Chem. Phys.* **2010**, *211*, 28.

[98] A. Pucci, F. Di Cuia, F. Signori, G. Ruggeri, *J. Mater. Chem.* **2007**, *17*, 783.

[99] F. Donati, A. Pucci, C. Cappelli, B. Mennucci, G. Ruggeri, *J. Phys. Chem. B* **2008**, *112*, 3668.

[100] F. Donati, A. Pucci, G. Ruggeri, *Phys. Chem. Chem. Phys.* **2009**, *11*, 6276.

[101] X. Jin, M. Götz, S. Wille, Y. K. Mishra, R. Adelung, C. Zollfrank, *Adv. Mater. (Weinheim, Ger.)* **2013**, *25*, 1342.

[102] S. N. Raja, A. C. K. Olson, K. Thorkelsson, A. J. Luong, L. Hsueh, G. Chang, B. Gludovatz, L. Lin, T. Xu, R. O. Ritchie, A. P. Alivisatos, *Nano Lett.* **2013**, *13*, 3915.

[103] J. N. Brantley, C. B. Bailey, K. M. Wiggins, A. T. Keatinge-Clay, C. W. Bielawski, *Polym. Chem.* **2013**, *4*, 3916.

[104] N. Bruns, K. Pustelny, L. M. Bergeron, T. A. Whitehead, D. S. Clark, *Angew. Chem., Int. Ed.* **2009**, *48*, 5666.

[105] N. Bruns, D. S. Clark, *Chimia* **2011**, *65*, 245.

[106] K. Makyła, C. Müller, S. Lörcher, T. Winkler, M. G. Nussbaumer, M. Eder, N. Bruns, *Adv. Mater. (Weinheim, Ger.)* **2013**, *25*, 2701.

[107] S. Lörcher, T. Winkler, K. Makyła, C. Ouellet-Plamondon, I. Burgert, N. Bruns, *J. Mater. Chem. A* **2014**, *2*, 6231.

[108] J. N. Brantley, C. B. Bailey, J. R. Cannon, K. A. Clark, D. A. Vanden Bout, J. S. Brodbelt, A. T. Keatinge‑Clay, C. W. Bielawski, *Angew. Chem., Int. Ed.* **2014**, *53*, 5088.

[109] J. Longo, C. Yao, C. Rios, N. T. T. Chau, F. Boulmedais, J. Hemmerlé, P. Lavalle, S. M. Schiller, P. Schaaf, L. Jierry, *Chem. Commun.* **2015**, *51*, 232.

[110]   E. M. Nofen, N. Zimmer, A. Dasgupta, R. Gunckel, B. Koo, A. Chattopadhyay, L. L. Dai, *Polym. Chem.* **2016**, *7*, 7249.

[111]   Z. a. Li, R. Toivola, F. Ding, J. Yang, P.-N. Lai, T. Howie, G. Georgeson, S.-H. Jang, X. Li, B. D. Flinn, A. K. Y. Jen, *Adv. Mater. (Weinheim, Ger.)* **2016**, *28*, 6592.

[112]   R. Toivola, P.-N. Lai, J. Yang, S.-H. Jang, A. K. Y. Jen, B. D. Flinn, *Compos. Sci. Technol.* **2017**, *139*, 74.

[113]   A. Ruiz de Luzuriaga, J. M. Matxain, F. Ruiperez, R. Martin, J. M. Asua, G. Cabanero, I. Odriozola, *J. Mater. Chem. C* **2016**, *4*, 6220.

[114]   J. Zou, Y. Liu, B. Shan, A. Chattopadhyay, L. Dai, L., *Smart Mater. Struct.* **2014**, *23*, 095038.

[115]   J. Zou, Y. Liu, A. Chattopadhyay, L. Dai, *Proc. SPIE* **2015**, *9432*, 943204.

[116]   M. N. Elizabeth, W. Jason, K. Bonsung, C. Aditi, L. D. Lenore, *Mater. Res. Express* **2016**, *3*, 035701.

[117]   E. M. Nofen, A. Dasgupta, N. Zimmer, R. Gunckel, B. Koo, A. Chattopadhyay, L. L. Dai, *Polym. Eng. Sci.* **2017**, *57*, 901.

[118]   H. Dietz, M. Rief, *Proc. Natl. Acad. Sci. U. S. A.* **2004**, *101*, 16192.

[119]   R. Perez-Jimenez, S. Garcia-Manyes, S. R. K. Ainavarapu, J. M. Fernandez, *J. Biol. Chem.* **2006**, *281*, 40010.

[120]   M. Bertz, A. Kunfermann, M. Rief, *Angew. Chem., Int. Ed.* **2008**, *47*, 8192.

[121]   A. P. Esser-Kahn, M. B. Francis, *Angew. Chem., Int. Ed.* **2008**, *47*, 3751.

[122]   J. Saeger, V. P. Hytönen, E. Klotzsch, V. Vogel, *PloS one* **2012**, *7*, e46962.

[123]   W. Rähse, *ChemBioEng Rev.* **2014**, *1*, 27.

[124]   A. Scott, *Chem. Eng. News* **2017**, *95*, 18.

[125]   J. W. Woodcock, R. Beams, C. S. Davis, N. Chen, S. J. Stranick, D. U. Shah, F. Vollrath, J. W. Gilman, *Adv. Mater. Interfaces* **2017**, *4*, 1601018.

[126]   T. Kosuge, K. Imato, R. Goseki, H. Otsuka, *Macromolecules* **2016**, *49*, 5903.

[127]   K. Imato, J. C. Natterodt, J. Sapkota, R. Goseki, C. Weder, A. Takahara, H. Otsuka, *Polym. Chem.* **2017**, *8*, 2115.

[128]   Y. Fang, K. Wang, D. Hui, F. Xu, W. Liu, S. Yang, L. Wang, *Compos. Part B: Eng.* **2017**, *112*, 93.

[129]   L. S. Schadler, S. C. Giannaris, P. M. Ajayan, *Appl. Phys. Lett.* **1998**, *73*, 3842.

[130]   J. Harding, L. M. Welsh, *J. Mater. Sci.* **1983**, *18*, 1810.

[131]   M. Rumsey, A., J. A. Paquette, *Proc. SPIE* **2008**, *6933*, 69330E.

[132]   G. Zhou, L. M. Sim, *Smart Mater. Struct.* **2002**, *11*, 925.

[133]   J. Wen, Z. Xia, F. Choy, *Compos. Part B: Eng.* **2011**, *42*, 77.

[134]   L. Gao, E. T. Thostenson, Z. Zhang, T.-W. Chou, *Adv. Funct. Mater.* **2009**, *19*, 123.

[135]   L. Gao, T.-W. Chou, E. T. Thostenson, Z. Zhang, M. Coulaud, *Carbon* **2011**, *49*, 3382.

[136]   J. Zhang, J. Liu, R. Zhuang, E. Mäder, G. Heinrich, S. Gao, *Adv. Mater. (Weinheim, Ger.)* **2011**, *23*, 3392.

[137]   S.-l. Gao, R.-C. Zhuang, J. Zhang, J.-W. Liu, E. Mäder, *Adv. Funct. Mater.* **2010**, *20*, 1885.

[138]   J. Zhang, R. Zhuang, J. Liu, E. Mäder, G. Heinrich, S. Gao, *Carbon* **2010**, *48*, 2273.

[139]   S. Luo, W. Obitayo, T. Liu, *Carbon* **2014**, *76*, 321.

[140]   J. Karger-Kocsis, H. Mahmood, A. Pegoretti, *Prog. Mater. Sci.* **2015**, *73*, 1.

[141]   R. F. Gibson, *Compos. Struct.* **2010**, *92*, 2793.

[142]   M. Lin, F.-K. Chang, *Compos. Sci. Technol.* **2002**, *62*, 919.

[143]   J. F. Fernandez, A. Dogan, Q. M. Zhang, J. F. Tressler, R. E. Newnham, *Sens. Actuators, A* **1995**, *51*, 183.

[144]   Y. Lin, H. A. Sodano, *Compos. Sci. Technol.* **2008**, *68*, 1911.

[145]   Y. Lin, H. A. Sodano, *Adv. Funct. Mater.* **2009**, *19*, 592.

[146]   M. D. Todd, J. M. Nichols, S. T. Trickey, M. Seaver, C. J. Nichols, L. N. Virgin, *Philos. Trans. R. Soc., A* **2007**, *365*, 317.

[147]   M. Majumder, T. K. Gangopadhyay, A. K. Chakraborty, K. Dasgupta, D. K. Bhattacharya, *Sens. Actuators, A* **2008**, *147*, 150.

[148]   M. Islam, M. Ali, M.-H. Lai, K.-S. Lim, H. Ahmad, *Sensors* **2014**, *14*, 7451.

[149]   S.-W. Kim, E.-H. Kim, M.-S. Jeong, I. Lee, *Compos. Part B: Eng.* **2015**, *74*, 13.

[150]   C.-S. Shin, S.-K. Liaw, S.-W. Yang, *Sensors* **2014**, *14*, 4144.

[151]   E. W. Steve, A. Farhad, D. Rohit, K. Chandrashekhara, C. W. Donald, *Smart Mater. Struct.* **2007**, *16*, 515.

[152]   S.-P. Julián, G. Alfredo, E. M. Luis, *Smart Mater. Struct.* **2013**, *22*, 025011.

[153]   G. F. Pereira, L. P. Mikkelsen, M. McGugan, *PloS one* **2015**, *10*, e0141495.

[154]   F. Li, H. Murayama, K. Kageyama, T. Shirai, *Sensors* **2009**, *9*, 4005.

[155]   D. Kinet, P. Mégret, K. Goossen, L. Qiu, D. Heider, C. Caucheteur, *Sensors* **2014**, *14*, 7394.

[156]   Z.-S. Guo, J. Zhang, H. Hu, X. Guo, *Proc. SPIE* **2007**, *6423*, 64230I.

[157]   S. Kerstin, E. Wolfgang, A. Jörg, L. Elfrun, L. Gerhard, *Meas. Sci. Technol.* **2006**, *17*, 1167.

[158]   S. Tian, Z. Yang, X. Chen, Y. Xie, *Sensors* **2015**, *15*, 19992.

[159]   J. Sierra-Pérez, M. A. Torres-Arredondo, A. Güemes, *Compos. Struct.* **2016**, *135*, 156.

[160]   A. Lamberti, G. Chiesura, G. Luyckx, J. Degrieck, M. Kaufmann, S. Vanlanduit, *Sensors* **2015**, *15*, 27174.

[161]   Y. M. Gebremichael, W. Li, W. J. O. Boyle, B. T. Meggitt, K. T. V. Grattan, B. McKinley, G. F. Fernando, G. Kister, D. Winter, L. Canning, S. Luke, *Sens. Actuators, A* **2005**, *118*, 78.

[162]   M. W. Nielsen, J. W. Schmidt, J. H. Høgh, J. P. Waldbjørn, J. H. Hattel, T. L. Andersen, C. M. Markussen, *J. Compos. Mater.* **2014**, *48*, 365.

[163]   C. A. Galindez-Jamioy, J. M. López-Higuera, *J. Sens.* **2012**, *2012*, Article ID 204121.

[164]   X. Bao, L. Chen, *Sensors* **2012**, *12*, 8601.

[165]   T. Horiguchi, T. Kurashima, M. Tateda, *IEEE Photonics Technol. Lett.* **1989**, *1*, 107.

[166]   D. Culverhouse, F. Farahi, C. N. Pannell, D. A. Jackson, *Electron. Lett.* **1989**, *25*, 913.

[167]   S. Minakuchi, N. Takeda, S.-i. Takeda, Y. Nagao, A. Franceschetti, X. Liu, *Compos. Part A: Appl. Sci. Manufact.* **2011**, *42*, 669.

[168]   B.-H. Choi, D.-C. Seo, I.-B. Kwon, *Compos. Sci. Technol.* **2017**, *142*, 264.

[169]   M. Hu, S. Peil, Y. Xing, D. Dohler, L. Caire da Silva, W. H. Binder, M. Kappl, M. B. Bannwarth, *Mater. Horiz.* **2018**.

[170]   Y. K. Song, B. Kim, T. H. Lee, S. Y. Kim, J. C. Kim, S. M. Noh, Y. I. Park, *Sens. Actuators, B* **2017**, *accepted manuscript*, https://doi.org/10.1016/j.snb.2017.11.019.

[171]   A. R. Hamilton, N. R. Sottos, S. R. White, *J. R. Soc. Interface* **2011**.

[172]   K. R. Hart, S. M. Lankford, I. A. Freund, J. F. Patrick, B. P. Krull, E. D. Wetzel, N. R. Sottos, S. R. White, *Compos. Sci. Technol.* **2017**, *151*, 1.

[173]   A. Kousourakis, A. P. Mouritz, M. K. Bannister, *Compos. Struct.* **2006**, *75*, 610.

[174]   A. R. Hamilton, N. R. Sottos, S. R. White, *Exp. Mech.* **2010**, *50*, 255.

[175]   G. R. Gossweiler, T. B. Kouznetsova, S. L. Craig, *J. Am. Chem. Soc.* **2015**, *137*, 6148.

[176]   X. Bao, D. J. Webb, D. A. Jackson, *Opt. Lett.* **1994**, *19*, 141.

[177]   X. Bao, C. Huang, X. Zeng, A. Arcand, P. Sullivan, *Opt. Eng.* **2002**, *41*, 1496.

[178]   H. Guo, G. Xiao, N. Mrad, J. Yao, *Sensors* **2011**, *11*, 3687.

[179]   C. Calvino, A. Guha, C. Weder, S. Schrettl, *Adv. Mater. (Weinheim, Ger.)* **2017**, accepted.

[180]   N. P. Avdelidis, C. Ibarra-Castanedo, X. P. V. Maldague, *Proc. SPIE* **2013**, *8705*, 87050G.